Electric Field Enhancement during Voltage Polarity Reversals in Lapped HVDC Cables

Electric Field Enhancement during Voltage Polarity Reversals in Lapped HVDC Cables

Bassel Diban
Department of Electrical, Electronic and Information Engineering (DEI)
University of Bologna
Bologna, Italy
bassel.diban2@unibo.it

Giovanni Mazzanti
Department of Electrical, Electronic and Information Engineering (DEI)
University of Bologna
Bologna, Italy
giovanni.mazzanti@unibo.it

Antonio Battaglia
TERNA
Via Benigni 21
00156 Roma, Italy
antonio.battaglia@terna.it

Massimo Marzinotto
TERNA
Via Benigni 21
00156 Roma, Italy
massimo.marzinotto@terna.it

***Abstract*—This paper aims at investigating the effect of fast and slow Voltage Polarity Reversals (VPRs) on the electric field distribution inside the insulation thickness of lapped cables. Two types of lapped cables, i.e., oil-filled cables and Mass Impregnated Non-draining (MIND) cables are investigated. The results show that fast VPRs lead to the greatest field enhancement during the transient. The longer the relaxation period during the slow VPRs, the lesser the fatigue applied on the insulation. Oil-filled cables have greater field enhancement during VPRs, while in MIND cables the transient lasts longer.**

Keywords—HVDC transmission, power cables, cable insulation, Power system transient, Electric fields.

I. Introduction

High Voltage Direct-Current HVDC systems have recently gained more attention, especially, with the boom in the renewable energy and the distributed generation [1], [2]. Although extruded cables have dominated the recent HVDC cable system projects, the lapped cables are still showing a reliable operation so far, especially Mass Impregnated Non-Draining (MIND) cables. The main disadvantage of MIND cables is their vulnerability to both high temperatures and load cycles, which might cause oil migration and contraction voids. However, MIND cables show high resilience when subjected to electrical transients compared to extruded insulations. For this reason, all HVDC projects with Line Commutated Converters (LCC) were conceived for use MIND cables (except Hokkaido-Honshu link in Japan [1]), since Voltage Polarity Reversal (VPR) is necessary to reverse power flow direction in this configuration [1]. However, the possible refurbishment of current LCC systems with extruded cables justifies also the development of extruded cables which are able to withstand VPRs [3]; as an example, the refurbished land section of IFA 2000 is an extruded HVDC cable used with LCC technology [4]. While VPRs in Cross-linked Polyethylene (XLPE) have already been investigated in [5], this study aims at studying the effect of both fast and slow VPRs on the electric field distribution inside lapped cable insulation.

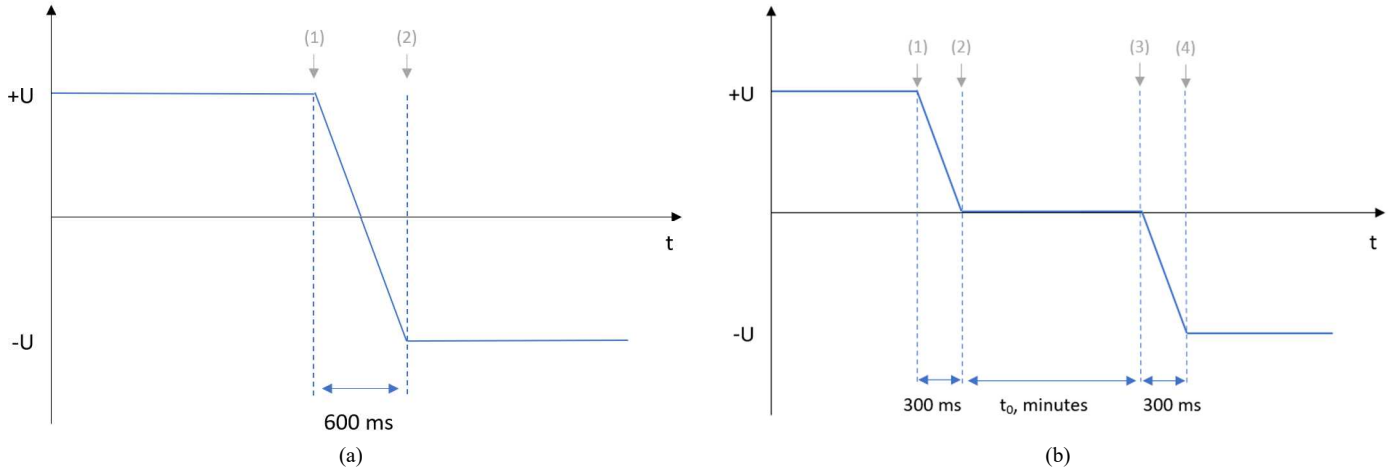

Fig. 1. Voltage wave shape over time in (a) fast polarity reversal and (b) slow polarity reversal [6].

II. Case Study

A. Voltage Polarity Reversals

VPRs are of two types (as shown in Fig. 1):

- Fast VPRs: (as in Fig. 1a) in this event, the polarity of the applied voltage is reversed within few hundreds of ms. The current is still flowing in the cable in same direction, hence, the cable is still hot and there is no transient in the temperature [7], [8]. This type of VPRs is only used during contingencies in the power grid to keep its frequency within its operating limits.
- Slow VPRs: (as in Fig. 1b) in this case, the voltage is switched off within hundreds of ms, followed by a charge relaxation period t_0 lasting some minutes, whereby both the voltage and current are set to zero. Then the voltage is switched on again with an opposite polarity. Here, the temperature is reduced during the relaxation period as reported in section II-E. This type of VPRs is used more frequently to meet the market needs [6]. However, also slow VPRs are setting some challenge to cable insulation, therefore also the number of slow VPRs permitted over cable life is limited according to manufacturers' prescriptions, although not so strictly as fast VPRs. Despite such limitation, TSOs are striving to increase the number of slow VPRs to follow market needs as closely as possible.

B. Electric Field Calculation:

The electric field is calculated inside the insulation thickness by solving Maxwell's Equations (1) – (3) beside the macroscopic conductivity equation (4) [9]:

$$\nabla \cdot (\varepsilon_0 \varepsilon_r \boldsymbol{E}) = \rho \quad (1)$$

$$\nabla \cdot \boldsymbol{J} = -\partial\rho/\partial t \quad (2)$$

$$\boldsymbol{J} = \sigma \boldsymbol{E} \quad (3)$$

$$\sigma = \sigma_0 \, exp(aT + bE) \quad (4)$$

where $\boldsymbol{E}$ is the electric field vector [V/m], ε_0=8.854×10^{-12} [F/m] is the vacuum permittivity, ε_r is the relative permittivity of the insulation, $\boldsymbol{J}$ is the direct conduction current density vector [A/m^2], ρ is the free charges density [C/m^3], σ is the conductivity [S/m], σ_0 is the conductivity at the reference values of the temperature and the electric field T_0 and E_0, respectively. a is the temperature coefficient of electrical conductivity ($°C^{-1}$ or K^{-1}), b is the field coefficient of electrical conductivity (mm/kV or m/MV). The insulation thickness is divided into 25 equally distributed layers for the Finite Difference Method FDM which is applied in MATLAB environment.

C. Cable Characteristics

The cable investigated in this paper is a 500 kV land lapped cable. Table I shows the main characteristics and geometries of the case-study cable.

TABLE I
Parameters of The Case-study Cable

Parameter	Value	
Insulation Type	Oil-filled OF	Mass Impregnated Non-draining MIND
Rated power (bipolar scheme) [MW]	1879	1425
Rated voltage, U_0 [kV]	500	500
Rated current, I_n [A]	1879	1425
Conductor Material	Cu	Cu
relative permittivity ε_r	3.5	3.5
$tan\ \delta$	0.01	0.01
Design temperature T_D [°C]	85	55
Ambient temperature [°C]	20	20
Conductor cross-section [mm^2]	1600	1600
Inner semiconductor thickness [mm]	2	2
Insulation thickness [mm]	21.74	21.74
Outer semiconductor thickness [mm]	1	1
Metallic shield thickness [mm]	1	1
Thermoplastic sheath thickness [mm]	4.5	4.5
Burial depth [m]	1.3	1.3
Thermal resistivity of the insulation [m.K/W]	5	6
Design value of soil resistivity [m.K/W]	1.3	1.3

For the sake of comparison, two types of insulation for lapped HVDC cables are chosen here, namely:

i) kraft paper impregnated with low-viscosity oil. In this case, the field and temperature coefficients of conductivity, a and b, are chosen as in [10];
ii) mass impregnated non-draining insulation, where Kraft paper is impregnated with high-viscosity oil to avoid oil leakage. In this case, a and b, are chosen as in [11].

Actually, the data of conductivity coefficients a and b date back to 15 years [10] and 25 years [11], respectively for OF and MIND cables. It is hard to find updated data in the literature, as such data are mostly confidential and known to manufacturers only, while the data reported here come from milestone papers and were often used in subsequent papers. Moreover, the main focus here is illustrating the calculation methodology, in addition to the particular quantitative results obtained. Table II presents the considered values of a and b.

TABLE II
Coefficients of Electrical Conductivity

Parameter	Value	
	OF	MIND
Temperature coefficient of electrical conductivity a (1/°C)	0.074	0.1
Field coefficient of electrical conductivity b (mm/kV)	0.3	

D. Temperature Transients:

The transient temperature profile is calculated according to the transient thermal model of cable layers as well as its surrounding environment as prescribed in IEC Standard 60853-2 [12]. Detailed description of the transient temperature profile

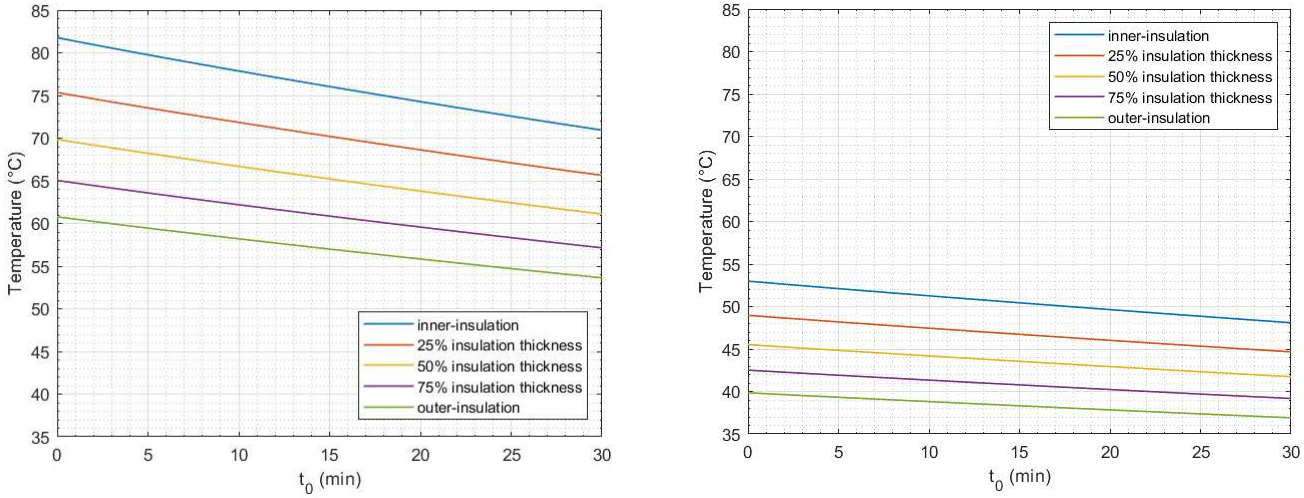

Fig. 2. Temperature distribution in 5 points of the insulation thickness during 30 minutes of the relaxation period t_0 of slow VPRs for (a) Oil-filled cable and (b) MIND cable.

calculations with all equations can be found in [13]. The VPR is assumed to occur after 24 hours of the energization and loading of the cable, to be sure that the cable has already reached both electrical and thermal stability at the instant of the VPR. In the case of slow VPRs, the natural cooling of the cable is also considered for the sake of accuracy of the simulation results, as shown in Fig. 2: two different temperature profiles are considered in the simulations for oil-filled and MIND cables, since the former has a higher maximum operating temperature on the conductor (85°C, see Fig. 2(a)) than the latter (55°C, see Fig. 2(b)).

E. Dielectric time constant and relaxation times

As far as the electric field transients are concerned, it is worth introducing the time constant of the dielectric in (5):

$$\tau = \varepsilon/\sigma = \varepsilon_0\varepsilon_r/\sigma \qquad (5)$$

The time constant is related to the non-linear conductivity which varies with the temperature and the electric field according to the values of a and b. Therefore, different values of the time constant will characterize oil-filled HVDC cables vs. MIND HVDC cables, which feature different values of a and b, as well as different values of maximum operating temperature (see Figs. 2(a) and (b)). For this reason, different values of relaxation time t_0 are considered in this study, namely, 2, 10, and 30 minutes. With reference to these values, it should be emphasized that in the current operational practice, t_0 lasts few minutes, [6], with the tendency to reduce it as much as possible – e.g. 2 min – in order to follow the electricity market as closely as possible; however, here much longer values of t_0 are also analyzed – depending also on the time constant of the dielectric – in order to seek the full relaxation of charges corresponding to the full stabilization of electric field profiles.

III. Results and Discussion

Fig. 3 shows the transient electric field distribution inside the insulation thickness calculated from (1) – (4) of oil-filled cable for (Fig. 3a) fast VPR, (Fig. 3b) slow VPR with t_0=2 min, (Fig. 3c) slow VPR with t_0=10 min, (Fig. 3d) slow VPR with t_0=30 min. It is worth highlighting that first instant of all curves (the blue curve) is considered to be at the hour 24 after the voltage application and loading the cable. Hence, the cable has already reached the resistive electric field distribution. The dashed curves represent the electric field during the transients lasting few hundreds of milliseconds, i.e., from (1) to (2) and/or from (3) to (4) in Fig. 1. The dot-dashed curves are the field distributions during t_0 of the slow VPRs. Fig. 3a shows the greatest electric field enhancement after VPR, as no charge relaxation takes place. In Fig. 3b (t_0=2 min) the maximum electric field is relaxed to ≈11 kV/mm. The latter becomes ≈4 kV/mm for t_0=10 min (Fig. 3c) and ≈1 kV/mm for t_0=30 min (Fig. 3d). All Figures show that the relaxation at the inner insulation is faster than that at the outer insulation due to the higher temperature at the former compared to the latter, hence, the conductivity is higher according to (4) and the time constant is lower according to (5).

Fig. 4 shows the transient electric field distribution inside the insulation thickness of MIND cable for (Fig. 4a) fast VPR, (Fig. 4b) slow VPR with t_0=2 min, (Fig. 4c) slow VPR with t_0=10 min, (Fig. 4d) slow VPR with t_0=30 min. In this case, 2, 10, and 30 minutes of relaxation time t_0 cause a reduction in the field enhancement to 12 kV/mm, 7 kV/mm, and 3 kV/mm in the most stressed point (the inner insulation).

Comparing Fig. 3 and Fig. 4, it can be noticed that the field inversion in the MIND cable is lesser than that in the oil-filled cable – despite the higher temperature coefficient of the former vs. the latter – due to the smaller voltage drop within the insulation of MIND cable (Fig. 2a) vs. oil filled cable (Fig. 2a) [1],[11]. This leads to a field enhancement in the inner insulation of 14 kV/mm in MIND vs. 16 kV/mm in oil-filled cables. However, the relaxation in oil-filled cables is faster than that in

MIND cables because of the higher temperature, hence, the lesser time constant. Therefore, the oil-filled cable has a greater field peak during the VPR, while the MIND cable has a longer overstress period after the VPR.

Fig. 5 shows the dielectric time constant (in minutes) of 5 points inside the insulation thickness over time (in minutes) during t_0 – ranging from 0 to 30 minutes, see above - for (a) oil-filled cable and (b) MIND cable. The time constant increases during t_0 because of the reduction of both the temperature and the electric field (see Eq.(4) and (5)). The duration of the transient time is around 5τ, hence it is proportional to the time constant τ. While the inner-insulation (the most stresses point during the transient) has a lower time constant (≈8 minutes) in the oil-filled cable Fig. 5a, the same point of the insulation has a greater time constant (≈16 minutes) in the MIND cable, Fig. 5b. The former justifies the short relaxation period of the oil-filled cable and the latter justifies the long relaxation period of the MIND cable. The same result can be found by comparing Fig.4 with Fig.3. While the greatest field after the VPR reaches 48 kV/mm in the oil-filled cable, it can arrive to 46 kV/mm in the MIND cable. However, this might not necessarily mean that the stress is more critical in oil-filled cables, simply because the MIND cables have longer transient period. For this reason, further experimental verification is necessary to check the most critical case. Furthermore, an optimization of the value of a (as in [14]) depending on the electrothermal life model can give an optimized a as a compromise between the amplitude and the duration of the transient.

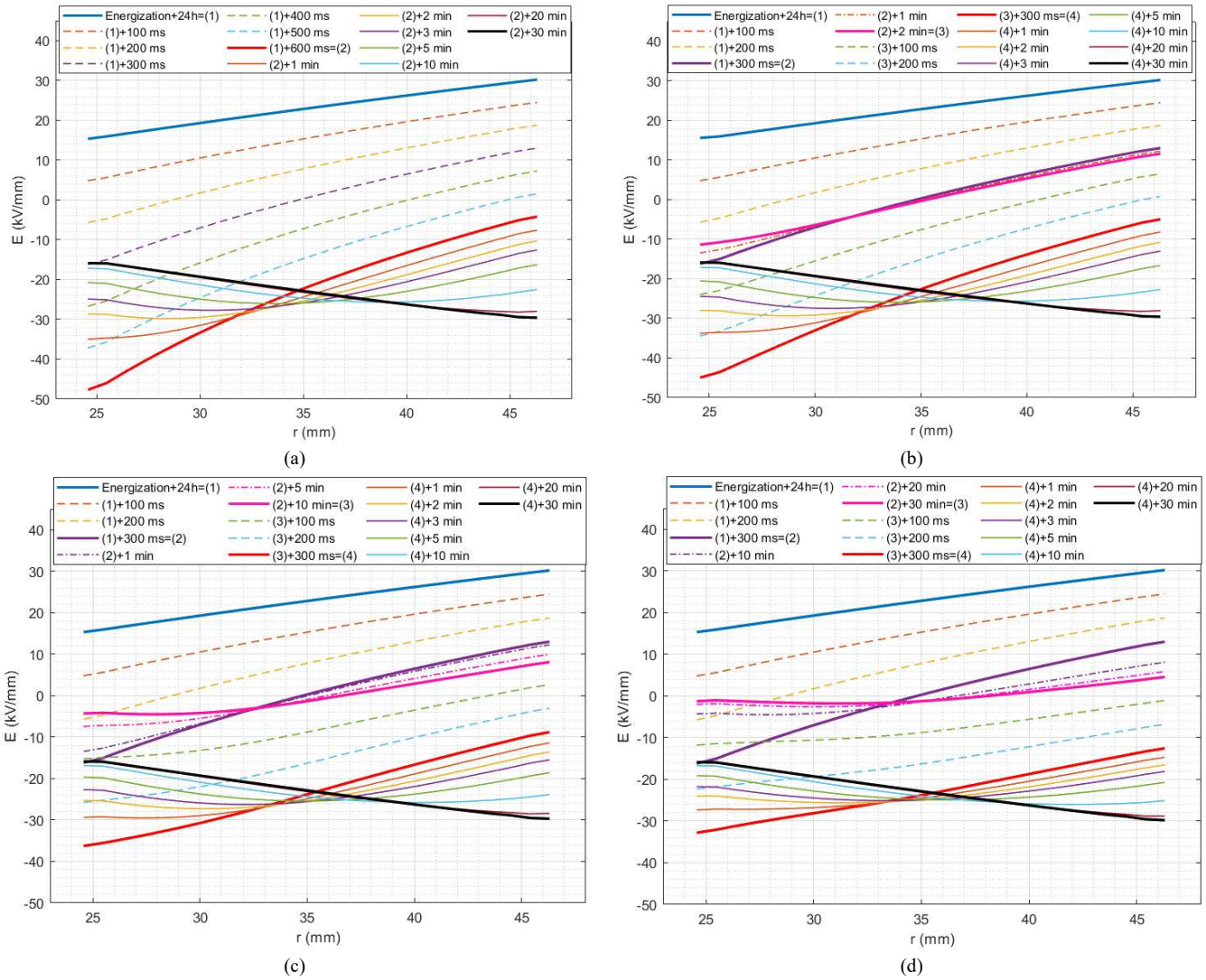

Fig. 3 Electric field distribution before, during, and after VPR in oil-filled cable insulation according to [10]:

(a) fast VPR
(b) slow VPR with t_0=2 min
(c) slow VPR with t_0=10 min
(d) slow VPR with t_0=30 min

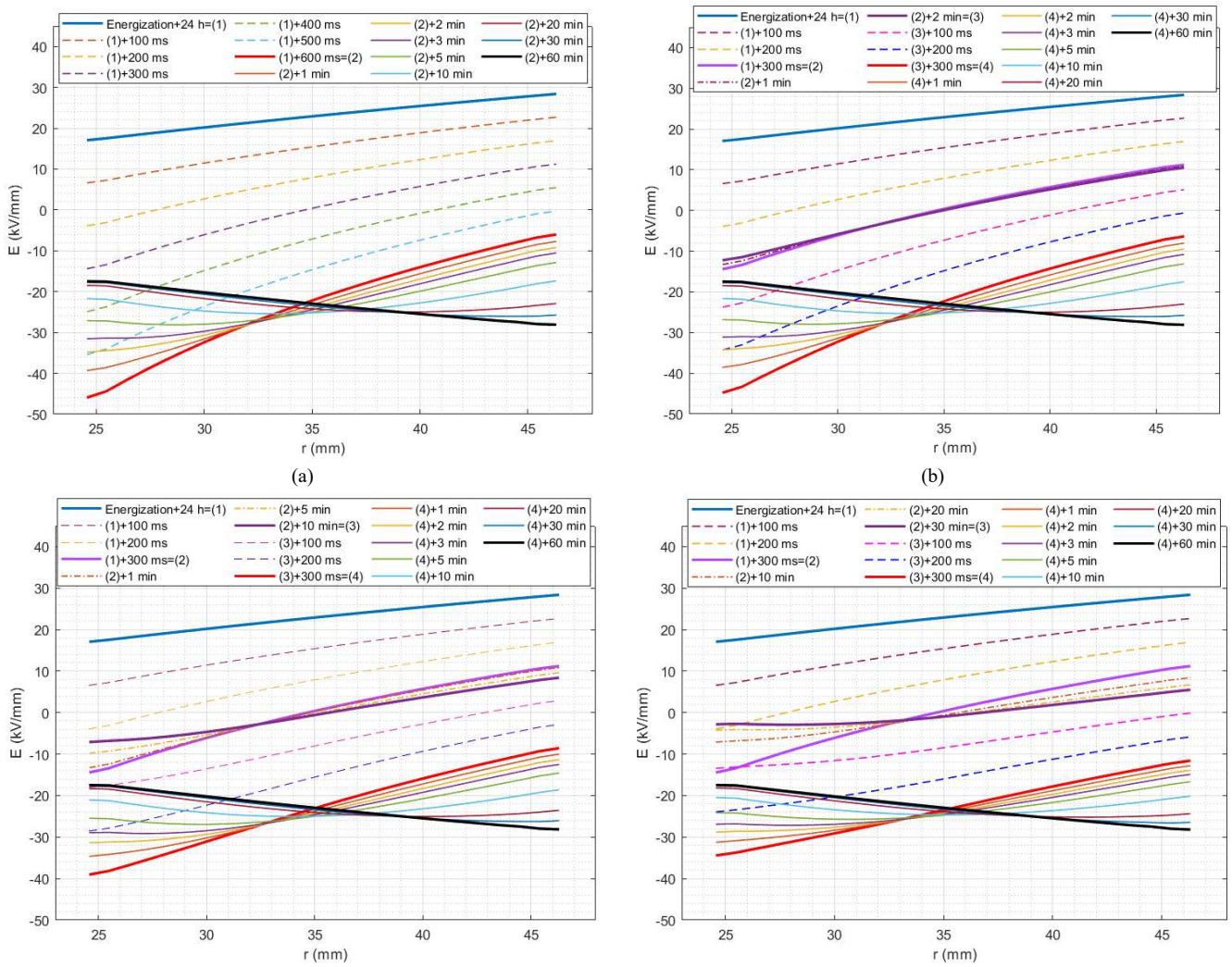

Fig. 4 Electric field distribution before, during, and after VPR in Mass Impregnated cable insulation according to [11]:
(a) fast VPR
(b) slow VPR with t_0=2 min
(c) slow VPR with t_0=10 min
(d) slow VPR with t_0=30 min

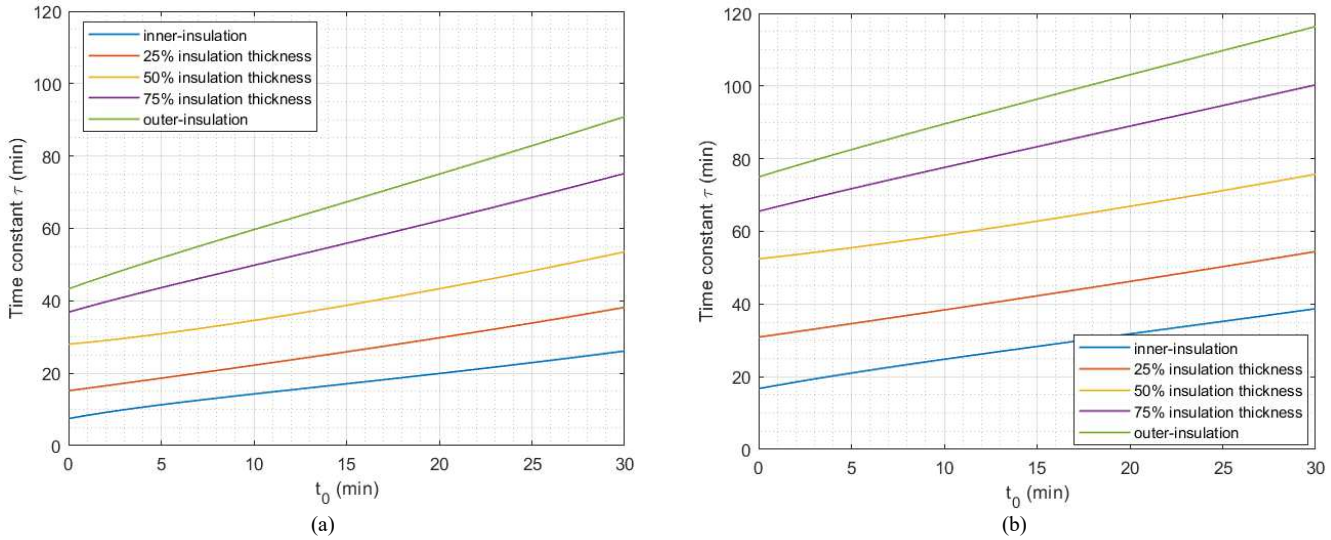

Fig. 5. Dielectric time constant (in minutes) of 5 points inside the insulation thickness over time (in minutes) during t_0 for (a) oil-filled cable and (b) MIND cable.

IV. Conclusion

The results obtained in this study show the way in which the VPRs overstress the insulation. Oil-filled cables have more field inversion and more field enhancement during VPRs compared to MIND cables. However, the transient of the VPR lasts shorter in OIL-field cables compared to MIND cables. While lower temperatures and/or values of conductivity coefficients lead to smaller peak of the electric field during VPRs, they cause a long-lasting effect of such small peaks. On the contrary, higher temperatures and/or values of conductivity coefficients lead to a greater peaks of the electric field which last shorter. Overall, fast VPRs show the greatest field enhancement. The longer the relaxation period during slow VPRs, the lesser the fatigue applied on the insulation. Further experimental verification and optimization of the conductivity coefficients are necessary to find a compromise between the amplitude and the duration of the VPR transients.

References

[1] G. Mazzanti and M. Marzinotto, *Extruded Cables For High-Voltage Direct-Current Transmission. Hoboken*, New Jersey: John Wiley & Sons, Inc., 2013.

[2] G. Mazzanti, “Issues and challenges for HVDC extruded cable systems,” Energies (MDPI), vol. 14, no. 15, pp. 1-34, 2021.

[3] M. Albertini, S. Cotugno, D. Pietribiasi and C. Remy, "HPTE Extruded Cables Polarity Reversals Performance in LCC HVDC Systems," 2020 AEIT International Annual Conference (AEIT), Catania, Italy, 2020, pp. 1-6.

[4] M. Mammeri, M. L. Paupardin, M. geneste, B. Dhuicq, “270 kV DC Extruded Land Cable Systems for LCC Power Transmission, “ the 10th International Conference on Insulated Power Cables, Jicable'19 - Paris - Versailles 23-27 June, 2019.

[5] B. Diban, G. Mazzanti, M. Marzinotto and A. Battaglia, "Electric Field Distribution after Polarity Reversal in HVDC Cables: The Effect of Insulation Characteristics," 2022 IEEE Conference on Electrical Insulation and Dielectric Phenomena (CEIDP), Denver, CO, USA, 2022, pp. 588-591.

[6] B. Diban, G. Mazzanti, M. Marzinotto, A. Battaglia, "Calculation of Electric Field Profile within HVDC Cable Insulation in the Presence of Voltage Polarity Reversals," in *IEEE Int. Conf. Dielectr. ICD 2022*, Palermo, 2022.

[7] G. Li, *et al.* “Power reversal strategies for hybrid LCC/MMC HVDC systems.,” *CSEE J. Power Energy Syst.*, *Vol*. 6, no. 1, pp. 203-21, 2020.

[8] H. Xiao, K. Sun, J. Pan, Y. Liu, “Operation and control of hybrid HVDC system with LCC and full-bridge MMC connected in parallel”. *IET Generation, Transmission & Distribution*, vol. *14*, no. 7, pp. 1344-1352, 2020.

[9] G. Mazzanti, "Including the calculation of transient electric field in the life estimation of HVDC cables subjected to load cycles," *IEEE Electr. Insul. Mag.*, vol. 34, no. 3, pp. 27-37, May-June 2018.

[10] R. N. Hampton, “Some of the considerations for materials operating under high-voltage, direct-current stresses,” IEEE Electr. Insul. Mag., vol. 24, no. 1, pp. 5–13, 2008.

[11] M. J. P. Jeroense and P. H. F. Morshuis, "Electric fields in HVDC paper-insulated cables," in IEEE Transactions on Dielectrics and Electrical Insulation, vol. 5, no. 2, pp. 225-236, April 1998.

[12] Calculation of the Cyclic and Emergency Current Rating of Cables, Part 2: Cyclic Rating of Cables Greater Than 18/30 (36) kV and Emergency Ratings for Cables of All Voltages, IEC 60853-2, Ed. 1.0, Jan. 1989.

[13] B. Diban, G. Mazzanti, “The Effect of Insulation Characteristics on Thermal Instability in HVDC Extruded Cables.,” *Energies* , Vol. *14*, pp.550, 2021.

[14] B. Diban, G. Mazzanti and P. Seri, "Life-Based Geometric Design of HVDC Cables—Part I: Parametric Analysis," in IEEE Transactions on Dielectrics and Electrical Insulation, vol. 29, no. 3, pp. 973-980, June 2022.